

Effects of Hydration and Dehydration on the Structure of Silica-Supported Vanadia Species

Shuibo Xie, Enrique Iglesia,* and Alexis T. Bell*

Chemical and Materials Sciences Divisions, Lawrence Berkeley National Laboratory and
Department of Chemical Engineering, University of California,
Berkeley, California 94720-1462

Received March 6, 2000. In Final Form: June 1, 2000

The effects of hydration and dehydration of silica-supported vanadia have been investigated with the aim of understanding how these processes alter the structure of the dispersed vanadia. Samples containing either 9 or 12 wt % V_2O_5/SiO_2 were examined by in situ Raman spectroscopy during hydration in 3 kPa water vapor at room temperature and during dehydration at temperatures between 298 and 773 K. The vanadia in freshly dehydrated 9 wt % V_2O_5/SiO_2 is present exclusively in the form of monovanadate species. Monovanadate species are predominant in the 12 wt % V_2O_5/SiO_2 , but a small amount of V_2O_5 is present as well. Room-temperature hydration causes a progressive loss of the Raman band at 1043 cm^{-1} , characteristic of isolated monovanadate species, and the gradual appearance of bands at 1021, 986, 895, 773, 706, 666, 512, 415, 325, 267, and 158 cm^{-1} , characteristic of a hydrated vanadia gel. Dehydration at elevated temperatures decomposes the gel and partially restores the presence of isolated monovanadate species. V_2O_5 particles are also formed during dehydration. Repeated low-temperature hydration and high-temperature dehydration leads to an irreversible conversion of isolated monovanadate species into V_2O_5 particles. A mechanism by which this process occurs is proposed.

Introduction

Supported vanadia catalysts exhibit high activity and selectivity for a number of oxidation reactions.^{1–3} These include the partial oxidation of methane^{4,5} and methanol to formaldehyde^{6–8} and the oxidative dehydrogenation ethane to ethene⁹ and propane to propene.^{10,11} Since the activity and selectivity of supported vanadia have been found to depend on the structure and distribution of the dispersed vanadia species, considerable effort has been devoted to the characterization of dispersed vanadia and their relationship to catalytic performance. Raman^{12–21}

infrared,^{12,13,22,23} UV–visible^{12,13,19,20,22,24} V NMR,¹⁷ and X-ray absorption^{25–29} methods have confirmed that, in the absence of water vapor, vanadium is present as three types of structures: isolated monovanadate (VO_4) species; polyvanadate species (chains and ribbons of VO_4 units); V_2O_5 crystallites. The distribution of vanadium among these structural types depends on the identity of the support, the composition of the vanadia precursor, the surface vanadia concentration, and the thermal history of the sample. At low vanadia surface densities vanadia ($<2.3\text{ VO}_x/\text{nm}^2$), monovanadate species are predominant on all supports. With increasing VO_x content, polyvanadate species are formed; on some supports, V_2O_5 crystallites also form. In general, TiO_2 , ZrO_2 , and Al_2O_3 support disperse VO_x species more effectively than SiO_2 , which forms crystalline V_2O_5 at surface densities well below those required for a polyvanadate monolayer ($\sim 7.5\text{ VO}_x/\text{nm}^2$).

The relationship of the structure of dispersed vanadia to its catalytic properties is illustrated by the following two examples. Investigations of methanol oxidation to formaldehyde have shown that the reaction requires

* To whom correspondence should be sent. E-mail: E.I., iglesias@cchem.berkeley.edu; A.T.B., bell@cchem.berkeley.edu.

(1) Albonetti, S.; Cavani, F.; Trifiro, R. *Catal. Rev.-Sci. Eng.* **1996**, *38*, 413.

(2) Blasko, T.; Lopez Nieto, J. M. *Appl. Catal.* **1997**, *157*, 117.

(3) Kung, H. H. *Adv. Catal.* **1994**, *40*, 1.

(4) Irusta, S.; Cornaglia, L. M.; Miro, E. E.; Lombardo, E. A. *J. Catal.* **1995**, *156*, 157.

(5) Sun, Q.; Jehng, J. M.; Hu, H. H.; Herman, R. G.; Wachs, I. E.; Klier, K. *J. Catal.* **1997**, *165*, 91.

(6) Kim, D. S.; Tatibouet, J. A.; Wachs, I. E. *J. Catal.* **1992**, *136*, 209.

(7) Deo, G.; Wachs, I. E.; Haber, J. *Crit. Rev. Surf. Chem.* **1994**, *40*, 1.

(8) Jeng, J.-M.; Hu, H.; Gao, X.; Wachs, I. E. *Catal. Today* **1996**, *28*, 335.

(9) Babares, M.; Gao, X.; Fierro, J. L. G.; Wachs, I. E. *Stud. Surf. Sci. Catal.* **1997**, *110*, 295.

(10) Khodakov, A.; Yang, J.; Su, S.; Iglesia, E.; Bell, A. T. *J. Catal.* **1997**, *177*, 343.

(11) Khodakov, A.; Olthof, B.; Bell, A. T.; Iglesia, E. *J. Catal.* **1999**, *181*, 205.

(12) Schraml-Marth, M.; Wokaun, A.; Pohl, M.; Krauss, H.-L. *J. Chem. Soc., Faraday Trans.* **1991**, *87*, 2635.

(13) Schraml-Marth, M.; Wokaun, A.; Pohl, M.; Krauss, H.-L. *J. Chem. Soc., Faraday Trans.* **1991**, *87*, 2635.

(14) Scharf, U.; Schraml-Marth, M.; Wokaun, A.; Baiker, A. *J. Chem. Soc., Faraday Trans.* **1991**, *87*, 3299.

(15) Roozeboom, F.; Mittelmeljer-Hazeleger, M. C.; Moulijn, J. A.; de Beer, V. H. J.; Gellings, P. J. *J. Phys. Chem.* **1980**, *84*, 2783.

(16) Went, G. T.; Oyama, S. T.; Bell, A. T. *J. Phys. Chem.* **1990**, *94*, 4240.

(17) Das, N.; Eckert, H.; Hu, H.; Wachs, I. E.; Walzer, J. F.; Feher, F. *J. Phys. Chem.* **1993**, *97*, 8240.

(18) Inamura, K.; Misono, M.; Okuhara, T. *Appl. Catal., A* **1997**, *149*, 133.

(19) Gao, X.; Bare, S. R.; Weckhuysen, B. M.; Waschs, I. E. *J. Phys. Chem.* **1998**, *102*, 10842.

(20) Olthof, B.; Khodakov, A.; Bell, A. T.; Iglesia, E. *J. Phys. Chem. B* **2000**, *104*, 1516.

(21) Bañares, M. A.; Cardoso, J. H.; Agulló-Rueda, F.; Correa-Bueno, J. M.; Fierro, J. L. G. *Catal. Lett.* **2000**, *64*, 191.

(22) Johnson, B.; Rebenstorf, B.; Larrson, R.; Andersson, S. L. *J. Chem. Soc., Faraday Trans. 1* **1988**, *84*, 1897.

(23) Inumaru, K.; Okuhara, T.; Misono, M. *J. Phys. Chem.* **1991**, *95*, 4826.

(24) Lische, G.; Hanke, W.; Jerschke, W. H. G.; Ohlmann, J. *J. Catal.* **1983**, *91*, 54.

(25) Yoshida, S.; Tanaka, T.; Nishimura, Y.; Mizutani, H.; Funabiki, T. *Proc. Int. Congr. Catal., 9th* **1988**, *3*, 1473.

(26) Tanaka, T.; Yamashita, H.; Tsuchitani, R.; Funabiki, T.; Yoshida, S. *J. Chem. Soc., Faraday Trans. 1* **1988**, *84*, 2987.

(27) Yoshida, S.; Tanaka, T.; Hanada, T.; Hiraiwa, T.; Kanai, H.; Funabiki, T. *Catal. Lett.* **1992**, *12*, 277.

(28) Takenaka, S.; Tanaka, T.; Yamazaki, T.; Funabiki, T.; Yoshida, S. *J. Phys. Chem.* **1997**, *101*, 9035.

(29) Inumaru, K.; Okuhara, T.; Misono, M.; Matsubayashi, N.; Shimada, H.; Nishijima, A. *J. Chem. Soc., Faraday Trans.* **1991**, *88*, 625.

isolated monovanadate species and proceeds with cleavage of the bond between the monovanadate species and the support (e.g., V–O–Si, V–O–Ti bond).^{19,30,31} By contrast, studies of the oxidative dehydrogenation of propane have shown that propene formation turnover rates per total V-atom increase with increasing VO_x surface density up to the point at which V₂O₅ crystallites form.^{10,11} This appears to reflect the higher reducibility and intrinsic activity of polyvanadates relative to monovanadate species. The ultimate decrease in turnover rate as VO_x surface density increases further reflects the loss of VO_x surface species as bulk V₂O₅ crystallites form.

Water is a common product of alkane and alcohol oxidation reactions. Because water can hydrolyze V–O–M (M = Si, Ti, Zr, etc.) bonds, the presence of water can influence the structure of dispersed vanadia species. A number of studies of this issue have been reported in the literature, the most detailed of which have been for the effects of H₂O on the dispersion of silica-supported vanadia.^{13,16,17,19,25–27} Raman and UV–visible spectra have shown that prolonged exposure to water vapor in ambient air causes the hydrolysis of V–O–Si bonds in isolated monovanadate species ((SiO₂)₃V=O) to form species resembling V₂O₅·*n*H₂O gels.^{32,33} It remains unclear, however, whether the subsequent dehydration of such gels can fully redisperse VO_x as isolated monovanadates or leads to the formation of V₂O₅ crystallites. The present study was undertaken in order to determine the dynamics and temperature dependence of the interaction of H₂O with VO_x/SiO₂, the species contributing to the formation of the hydrated V₂O₅·*n*H₂O gel, and the role of hydration/dehydration processes on the nucleation and growth of V₂O₅ crystallites.

Experimental Section

Two VO_x/SiO₂ samples were used in this study. A 9 wt % V₂O₅/SiO₂ sample was prepared by incipient-wetness impregnation of Cabosil EH-5 SiO₂ (dried at 393 K) with a solution of vanadium triisopropoxide (Alfa-Aesar; 97% purity) in 2-propanol.¹⁹ After impregnation, the sample was treated in flowing N₂ at 393 K for 1 h and then at 573 K for 1 h. A 12 wt % V₂O₅/SiO₂ catalyst was prepared by incipient wetness impregnation methods using a NH₄VO₃ aqueous solution. Ammonium metavanadate (Aldrich, 99%) was dissolved in a solution of oxalic acid (NH₄VO₃/oxalic acid molar ratio = 1:2) at a pH of 1.8. The sample was treated in 20% O₂/He (Bay Air; 40 cm³/min) in a quartz in-situ Raman cell. The sample temperature was raised from 298 to 773 K at 10 K/min and then held at 773 K for 2 h. The measured surface areas of the SiO₂ support and of the 12 wt % V₂O₅/SiO₂ sample after pretreatment in air at 773 K for 2 h were 350 and 238 m²/g, respectively.

Raman spectra were recorded using a HoloLab series 5000 Raman spectrometer (Kaiser Optical) equipped with a Nd:YAG laser that is frequency-doubled to 532 nm. The laser was operated at a power level of 30 mW measured at the sample with a power meter (Edmund Scientific). The resolution of the spectrometer is 5 cm⁻¹. Samples (~50 mg) were pressed into wafers at 35 MPa and placed within a rotary quartz Raman cell. The intensity of the Raman band for crystalline V₂O₅ depends on temperature (see discussion below); as a result, it was necessary to rotate the sample stage at 20 Hz in order to reduce laser heating of the samples. Hydration experiments were carried out using a 20% O₂/He mixture containing 3.0 kPa H₂O vapor, introduced by saturating the stream with liquid water at 298 K. After treatment with this mixture for a given time, the saturator was bypassed;

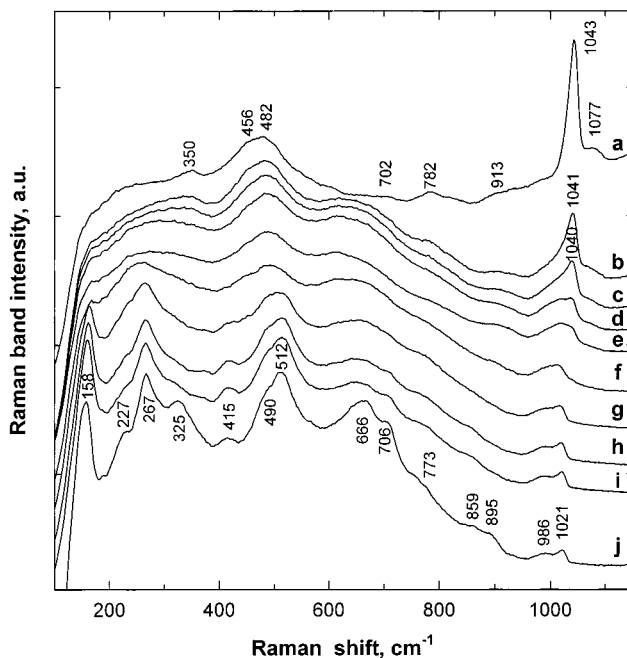


Figure 1. Raman spectra of freshly calcined 9 wt % V₂O₅ recorded at 298 K after exposure to 3.0 kPa H₂O for (a) 0 min, (b) 1 min, (c) 2 min, (d) 3 min, (e) 4 min, (f) 10 min, (g) 20 min, (h) 30 min, (i) 60 min, and (j) 12 h.

the sample was then flushed with dry 20% O₂/He and heated to 773 K at 10 K/min.

Results

Figure 1 shows the room-temperature spectrum for the 9 wt % V₂O₅/SiO₂ sample after treatment in 20% O₂/He at 773 K for 2 h (spectrum a). The sharp band at 1043 cm⁻¹ is characteristic of isolated monovanadate (VO₄),^{16,17,19,20} and the bands at 782, 482, and 350 cm⁻¹ correspond to the SiO₂ support.³⁴ The band at 1077 cm⁻¹ has been attributed to Si–O⁻ functionalities in silica produced by the formation of V–O–Si bonds.¹⁹

Exposure of the calcined sample to 3.0 kPa of H₂O at 298 K leads to an evolution in the structure of the supported vanadia as shown in Figure 1. The band at 1043 cm⁻¹ becomes weaker, and a weak broad band appears at ~1021 cm⁻¹ after about 10 min. At longer times, additional bands appear at 986, 895, 773, 706, 666, 512, 415, 325, 267, and 158 cm⁻¹. These new bands and the band at 1021 cm⁻¹ are consistent with the gradual formation of a V₂O₅·*n*H₂O gel. The Raman spectrum of V₂O₅·*n*H₂O gel formed by exposing V₂O₅ to H₂O vapor at room temperature exhibits bands at 1020 (w), 895 (s), 707 (s), 667 (m), 510 (m), 485 (sh), 400 (vw), 350 (m), 325 (m), 278 (w), 265 (m), 155 (s), and 135 (s).^{32,33}

Heating this hydrated 9 wt % V₂O₅/SiO₂ at 773 K for 1 h in 20% O₂/He restores the band at 1043 cm⁻¹, and new bands, corresponding to V₂O₅ crystallites, appear at 998, 704, 529, 483, 408, 305, 288, 199, and 147 cm⁻¹ (Figure 2). Subsequent hydration/dehydration cycles lead to the continuous growth of the V₂O₅ bands, without significant weakening of the band at 1043 cm⁻¹, corresponding to isolated monovanadates. To determine the amount of V₂O₅ formed after each hydration/dehydration cycle, it is necessary to know the relative Raman cross sections for V=O stretches in isolated monovanadate species and V₂O₅. These Raman cross sections were estimated by comparing

(30) Forzatti, P.; Tronconi, E.; Elmi, A. S.; Busca, G. *Appl. Catal.*, A **1997**, *157*, 387.

(31) Burcham, L. J.; Wachs, E. I. *Catal. Today* **1999**, *49*, 467.

(32) Abello, L.; Husson, E.; Repelin, Y.; Lucazeu, G. *Solid State Chem.* **1985**, *56*, 379.

(33) Repelin, Y.; Husson, E.; Abello, L.; Lucazeu, G. *Spectrochim. Acta* **1985**, *41A*, 993.

(34) Brinker, C. J.; Kirkpatrick, R. J.; Tallant, D. R.; Bunker, B. C.; Montez, B. J. *J. Non-Cryst. Solids* **1988**, *99*, 418.

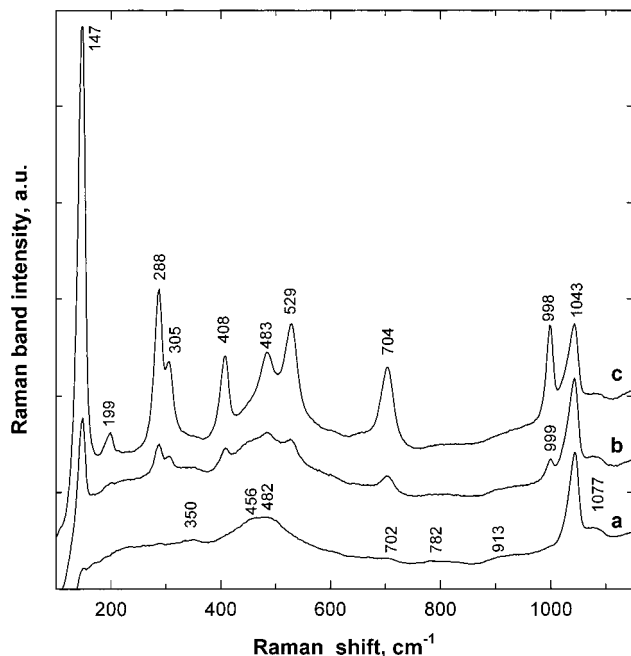


Figure 2. Raman spectra of 9 wt % V_2O_5/SiO_2 recorded at 298 K: (a) freshly calcined in 20% O_2/He ; (b) after dehydration in 3.0 kPa H_2O and dehydration for 1 h at 773 K in 20% O_2/He ; (c) after a second hydration/dehydration cycle identical to that used for (b).

the intensity of the band at 1043 cm^{-1} for the 9 wt % V_2O_5/SiO_2 sample (see Figure 1), which contains only monovanadate species, with the intensity of the band at 997 cm^{-1} for a physical mixture of bulk V_2O_5 and pure SiO_2 containing 9 wt % V_2O_5 . The V_2O_5 crystallites in this physical mixture have an average diameter of $\sim 0.5\ \mu\text{m}$. Assuming that the efficiency of sampling $V=O$ vibrations in the 9 wt % V_2O_5/SiO_2 sample and the sample containing 9 wt % bulk V_2O_5 mixed with SiO_2 are identical, the relative Raman cross sections for bulk V_2O_5 ($\nu_{V=O} = 997\text{ cm}^{-1}$) is estimated to be 10 times larger than that for isolated monovanadate species ($\nu_{V=O} = 1043\text{ cm}^{-1}$). Using this ratio of Raman scattering cross sections, an upper limit can be estimated for the fraction of the well-dispersed monovanadate species that are converted to V_2O_5 crystals after V_2O_5/SiO_2 has undergone a number of hydration/dehydration cycles. For the 9 wt % sample, less than 1% of the monovanadate species are converted to V_2O_5 after one hydration–dehydration cycle; this value approaches 10% after two cycles.

Spectrum a in Figure 3 was obtained after dehydration at 773 K for 1 h in 20% O_2/He of a fresh 12 wt % V_2O_5/SiO_2 sample that had been exposed to ambient air. Raman bands for both monovanadate species and V_2O_5 are clearly evident. The relative intensities of all bands are very similar to those for the 9 wt % V_2O_5/SiO_2 after two hydration/dehydration cycles (compare spectrum c in Figure 2 with spectrum a in Figure 3). Exposing the 12 wt % V_2O_5/SiO_2 sample to 3.0 kPa of water vapor at 298 K leads to a gradual change in the appearance of the spectrum (Figure 3). The band at 1043 cm^{-1} for the monovanadate species decreases in intensity, and it disappears completely after 10 min. The bands for bulk V_2O_5 at 998, 702, 528, 483, 406, 306, 285, 199, and 146 cm^{-1} also decrease in intensity with time. After 0.3 h, the spectrum changes gradually until spectrum k in Figure 3 is obtained after 1 h. This spectrum is again similar to that for 9 wt % V_2O_5/SiO_2 after the same treatment. These observations suggest that upon extended exposure to water

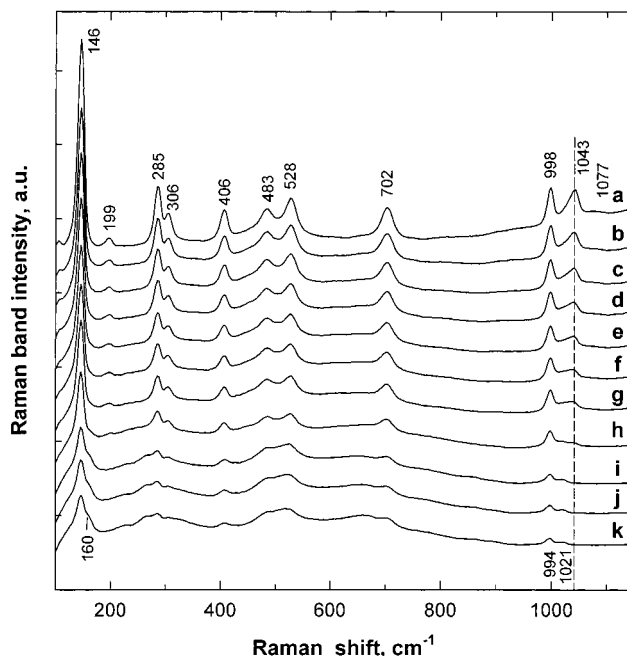


Figure 3. Raman spectra of calcined 12 wt % V_2O_5/SiO_2 recorded at 298 K after exposure to 3.0 kPa H_2O for (a) 0 min, (b) 0.5 min, (c) 1.0 min, (d) 1.5 min, (e) 2.0 min, (f) 2.5 min, (g) 3.0 min, (h) 10 min, (i) 20 min, (j) 30 min, and (k) 60 min.

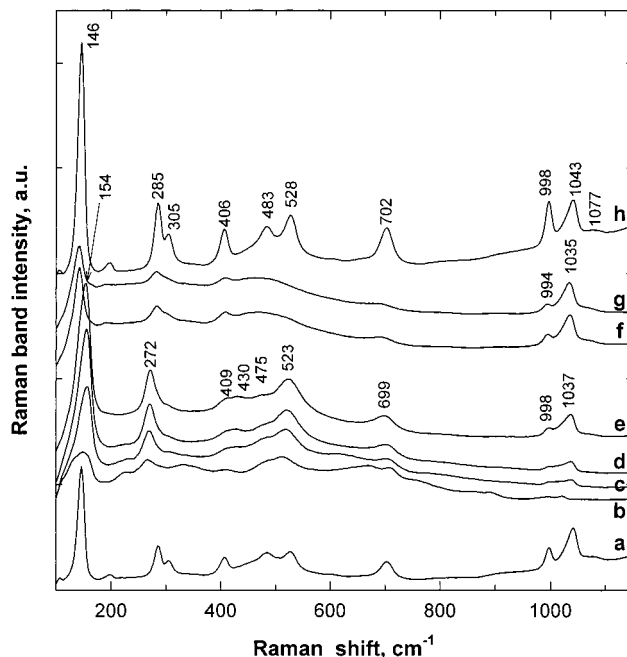


Figure 4. Raman spectrum of calcined 12 wt % V_2O_5/SiO_2 recorded at (a) 298 K, and Raman spectra of fully hydrated 12 wt % V_2O_5/SiO_2 recorded during dehydration for 1 h in flowing 20% O_2/He at (b) 298 K, (c) 393 K, (d) 473 K, (e) 573 K, (f) 673 K, (g) 773 K, and (h) 298 K after cooling the sample from 773 K.

vapor, both isolated monovanadate and supported V_2O_5 particles are converted to a hydrated vanadia gel.

The Raman spectra obtained during dehydration of the hydrated 12 wt % V_2O_5/SiO_2 samples are shown in Figure 4. Spectrum b was obtained after exposing the sample to 3 kPa of H_2O for 12 h. Spectra c–g show the changes that occur as the hydrated sample was heated to higher temperatures in 20% O_2/He . Each spectrum was recorded at the indicated temperature of treatment, which was maintained constant for 1 h before recording the spectrum.

During dehydration, the bands characteristic of a hydrated vanadia gel gradually disappear and bands for isolated vanadate species (1043 cm^{-1}) and for dispersed V_2O_5 (998 , 702 , 400 , and 146 cm^{-1}) reappear. Spectrum h was recorded after treatment at 773 K for 1 h and subsequent cooling to 298 K . The general appearance of the spectrum changes appreciably upon cooling the sample from 773 to 298 K , and the bands shift to slightly higher frequencies as the sample is cooled. All bands for V_2O_5 become more intense upon cooling, but the band for monovanadate species is unchanged. These effects of temperature on the intensity of Raman bands for V_2O_5 have been reported previously and are attributable to the formation of anionic defects in V_2O_5 crystallites at higher temperatures.³⁵ Absorption of both the incident and scattered light by defects within V_2O_5 crystallites causes a reduction in the sampling depth and, hence, a reduction in the intensity of the Raman signal observed for a given amount of V_2O_5 in the sample. The small increase in the Raman frequency with decreasing temperature reflects a small decrease in the $\text{V}=\text{O}$ bond length due to thermal contraction. The intensity of the peak at 1043 cm^{-1} is unaffected by temperature because the monovanadate species do not lose oxygen over the temperature range of the present experiments. There is a slight blue shift in the position of this band with decreasing temperature, due to $\text{V}=\text{O}$ bond contraction.

Figure 5A shows a plot of the intensities of the bands at 1043 and 998 cm^{-1} as a function of the number of hydration/dehydration cycles for the $12\text{ wt } \%$ $\text{V}_2\text{O}_5/\text{SiO}_2$ sample. The V_2O_5 band at 998 cm^{-1} grows significantly after two hydration/dehydration cycles, but the band at 1043 cm^{-1} remains unchanged. As the number of hydration/dehydration cycles increases, the band at 998 cm^{-1} becomes more intense and the band at 1043 cm^{-1} becomes weaker. The relative amounts of the two species can be calculated using the estimates of the relative cross sections for the two species, and they are shown in Figure 5B. For the fresh sample, about 3% of the vanadia in the sample is present as V_2O_5 , but after seven cycles, this value increases to 34% . The sigmoidal shape of the curve in Figure 5B indicates that the rate of the monovanadate conversion to V_2O_5 increases with number of cycles. This behavior may reflect an acceleration of the reaction rate once V_2O_5 nuclei of a critical size are formed. In contrast to what is observed upon low-temperature hydration and subsequent dehydration at elevated temperature, prolonged heating at 773 K in $20\% \text{ O}_2/\text{He}$ does not affect the distribution of isolated monovanadate species and V_2O_5 .

The effect of the temperature of exposure to H_2O was also examined. At 393 – 573 K , H_2O had no effect on the Raman spectrum of $12\text{ wt } \%$ $\text{V}_2\text{O}_5/\text{SiO}_2$ in agreement with previous observation.³⁶ Detectable structural changes occurred only upon water exposure at 353 K or lower temperatures. The slower kinetics observed for the monovanadate to V_2O_5 transformation at high temperatures may reflect a compromise between the adsorption of H_2O required for hydrolysis of $\text{V}-\text{O}-\text{Si}$ bonds, which is favored at low temperatures, and the rates of the hydrolysis and migration processes, which become faster as the temperature increases.

Discussion

The results of this study show that hydration (298 K)–dehydration (773 K) cycles cause the irreversible and

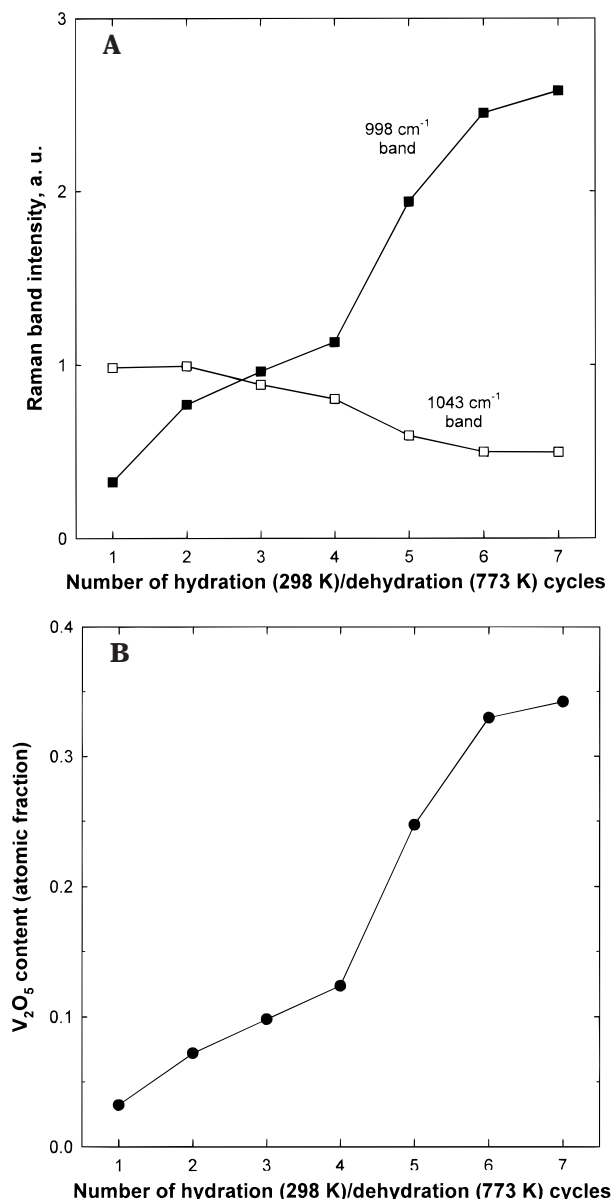


Figure 5. (A) Relative intensities of the Raman bands at 1043 and 998 cm^{-1} in the spectra recorded at 298 K for the $12\text{ wt } \%$ $\text{V}_2\text{O}_5/\text{SiO}_2$ plotted as a function of the number of hydration/dehydration cycles. (B) Fraction of V atoms present as V_2O_5 in the $12\text{ wt } \%$ $\text{V}_2\text{O}_5/\text{SiO}_2$ plotted as a function of the number of hydration/dehydration cycles.

gradual transformation of isolated monovanadate species into V_2O_5 crystallites on SiO_2 supports. A $\text{V}_2\text{O}_5/\text{SiO}_2$ sample with $9\text{ wt } \%$ V_2O_5 and a surface density of $1.9\text{ VO}_x/\text{nm}^2$ contains predominantly isolated monovanadate (Figure 1), in agreement with previous observations.¹⁹ The geometric “footprint” of a monovanadate species suggests that the saturation monovanadate coverage is about $2.3\text{ VO}_x/\text{nm}^2$,^{10,11,19} thus, the exclusive presence of monovanadate in this sample is not unexpected.

The surface density in the $\text{V}_2\text{O}_5/\text{SiO}_2$ sample with $12\text{ wt } \%$ V_2O_5 is $2.6\text{ VO}_x/\text{nm}^2$, and V_2O_5 bands are detected along with those for isolated vanadate species in the Raman spectrum. On the basis of estimates of the relative scattering cross sections for isolated monovanadate and crystalline V_2O_5 reported above, less than 3% of the V atoms in the sample are present as V_2O_5 (Figure 5B). It appears that V_2O_5 crystallites first form on SiO_2 as the theoretical monovanadate capacity of the SiO_2 surface is exceeded.

(35) Xie, S.; Iglesia, E.; Bell, A. T. To be submitted for publication.

(36) Jehng, J. M.; Deo, G.; Weckhuysen, B. M.; Wachs, I. E. *J. Mol. Catal., A* **1996**, *110*, 41.

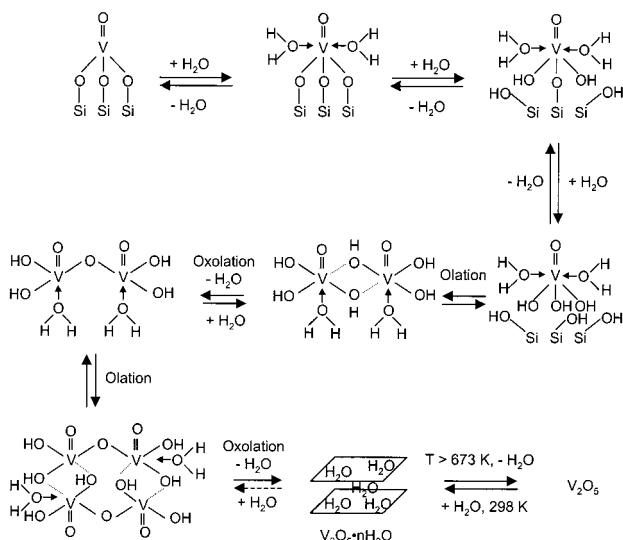


Figure 6. Proposed mechanism for the structural changes occurring during the hydration and dehydration of V_2O_5/SiO_2 .

The reaction of H_2O with monovanadate species is slow at room temperature (Figure 1), and it does not occur above 393 K when the partial pressure of H_2O is 3 kPa. Thus, it appears that the concentration of adsorbed water critically influences the restructuring process. In fact, if the enthalpy for water adsorption is greater than the activation energy for the hydrolysis or migration of monovanadate species, the rate of restructuring can actually decrease with increasing temperature.

The Raman spectra in Figure 1 show that, over ~ 0.5 h of hydration, the isolated vanadate species initially present on 9 wt % V_2O_5/SiO_2 are transformed into structures with Raman features similar to those in V_2O_5 gels formed by hydration of V_2O_5 crystallites. Similar effects were observed for the 12 wt % V_2O_5/SiO_2 sample (see Figure 3). In the latter sample, the small amounts of V_2O_5 present initially also form a hydrated V_2O_5 gel. The extent of V_2O_5 hydration appears to depend on the size of the V_2O_5 crystallites. As V_2O_5 crystallites become more abundant with repeated hydration/dehydration cycles, they do not undergo complete hydration at 298 K in 3 kPa of H_2O (see Figure 3). This may be due to the formation of progressively larger V_2O_5 crystallites that intercalate water with increasing difficulty. Indeed, the Raman spectrum of large unsupported crystallites in bulk V_2O_5 (~ 500 nm diameter) is unchanged by exposure to H_2O vapor at 298 K.

The reversibility of the structural effects of hydration depends also on the length of the hydration at 298 K. When either one of the V_2O_5/SiO_2 samples was exposed to 3 kPa of H_2O at 298 K for less than 10 min, subsequent dehydration in 20% O_2/He at 773 K completely restored the initial Raman spectrum and the isolated monovanadate species initially present in these samples. Dehydration after longer hydration times (> 10 min), however, led to the irreversible formation of V_2O_5 crystallites after repeated hydration/dehydration cycles (see Figures 2, 4, and 5).

Figure 6 depicts schematically the processes occurring during hydration/dehydration processes for VO_x species supported on SiO_2 . At 298 K, water is assumed to adsorb by interaction between the O-atom of H_2O and a V^{5+} center in isolated monovanadate species and by concurrent interactions of the H-atoms with neighboring O-atoms in $V-O-Si$ structures. These interactions are relatively weak and consequently H_2O desorbs slightly above room temperature. Near room temperature, the hydrolysis of

$V-O-Si$ bonds occurs slowly, as evidenced by the slow changes in the Raman spectrum of dispersed vanadia upon exposure of V_2O_5/SiO_2 samples to H_2O water vapor at 298 K (Figures 1 and 3). After all three $V-O-Si$ bonds in isolated monovanadate species have undergone hydrolysis, the resulting detached vanadyl trihydroxide species should be able to migrate on the silica surface and react with similar species via olation and oxolation processes to form $V-O(H)-V$ and $V-O-V$ bonds, respectively. These oligomerization processes lead to the formation of two-dimensional polyvanadate domains. As the degree of oxolation increases, these structures begin to resemble that of fully hydrated V_2O_5 , as suggested by Raman spectroscopy. Small crystallites of V_2O_5 (e.g., in 12 wt % V_2O_5/SiO_2), can also interact with water to form hydrated vanadia gels. While the hydrolysis of $V-O-Si$ bonds was not observed at 393 K in the presence of 3 kPa of H_2O , this does not exclude the possibility that, in the presence of higher H_2O partial pressures, hydrolysis could occur at elevated temperatures.

Dehydration of the two-dimensional polyvanadate species initially formed during the early stages of water exposure involves the cleavage of $V-O(H)-V$ bonds and the partial hydrolysis of $V-O-V$ bonds. The latter process would require the participation of adsorbed water, because water vapor is no longer available in the gas phase. Both processes can contribute to the re-formation of the vanadyl trihydroxide species required to redisperse the vanadia. Some of the two-dimensional structures continue to react with migrating trihydroxide species using on-top $V-OH$ groups away from the periphery of these domains; this leads to the formation of small three-dimensional structures, which continue to grow isotropically to form larger V_2O_5 crystallites. These small crystallites of V_2O_5 serve as nuclei for the additional formation of V_2O_5 during subsequent hydration–dehydration cycles. The nucleation and growth of V_2O_5 crystals causes the plot of V_2O_5 fraction as a function of the number of hydration–dehydration cycles (Figure 5B) to have a sigmoidal shape.

The interpretation of the effects of hydration and dehydration on silica-supported vanadia presented here differs from that developed by Gao et al.¹⁹ These authors have proposed that the formation of a hydrated vanadia gel can occur only when sufficiently large quantities of water are present to ensure that VO_x species are completely detached from the surface of silica. They have also suggested that once the gel is formed its dehydration does not lead to the redispersion of vanadia as isolated monovanadate species. The results reported here indicate that during dehydration a competition occurs between disaggregation of the vanadia gel to form isolated monovanadate species and crystallites of V_2O_5 . This suggests that the initially formed gel has regions in which the vanadium atoms are not fully linked to each other by $V-O-V$ bonds. It is hypothesized that such regions undergo hydrolytic cleavage of the $V-O-V$ bonds to form $V-OH$ groups and ultimately $OV(OH)_3$ species that can migrate along the silica surface. The regions of the gel that are more fully connected may serve as the nuclei for the formation of small V_2O_5 crystallites.

Conclusions

At surface densities below one monolayer ($2.3 VO_x/nm^2$) vanadia can be dispersed on the surface of silica exclusively as isolated monovanadate species. Above monolayer coverage small particles of V_2O_5 are observed. Low-temperature hydration of samples containing only isolated monovanadate species or a mixture of monovanadate

species and a small amount of V_2O_5 results in structural changes that are only partially reversible upon dehydration. Water vapor slowly hydrolyzes the V–O–Si bonds by which monovanadate species are bonded to the SiO_2 surface near room temperature. The resulting $O=V(OH)_3$ species then migrate to form two-dimensional structures via the processes of olation and oxolation. The Raman spectrum of this structure closely resembles that for fully hydrated V_2O_5 . If particles of V_2O_5 are present, they also undergo hydration to form a vanadia gel. Upon dehydration at elevated temperatures, the two-dimensional vanadia structure is destroyed. The V–O(H)–V bonds formed via olation are broken to form separate V–OH units, and the V–O–V bonds formed via oxolation undergo partial hydrolysis by reaction with bound water. These processes contribute to the generation of mobile $O=V(OH)_3$ species that can react with Si–OH groups on the silica surface to re-form the monovanadate groups. Oxolation

can also occur during dehydration leading to the formation of two-dimensional and ultimately three-dimensional V_2O_5 structures. Repeated low-temperature hydration/high-temperature dehydration of silica-supported vanadia results in the irreversible conversion of isolated monovanadate species to V_2O_5 particles. Hydrolysis of V–O–Si bonds is not observed upon water vapor exposure at elevated temperatures because of the low H_2O coverage on isolated monovanadate species.

Acknowledgment. The authors express their appreciation to Professor Israel E. Wachs of Lehigh University for supplying the 9 wt % V_2O_5/SiO_2 sample. This work was supported by the Director, Office of Basic Science, Chemical Sciences Division, of the U.S. Department of Energy under Contract DE-AC03-76SF00098.

LA0003342